

Aerodynamic Interference of Vertical Axis Wind Turbines

R. Ganesh Rajagopalan* and Ted L. Ricker†

Iowa State University, Ames, Iowa 50011

and

Paul C. Klimas‡

Sandia National Laboratories, Albuquerque, New Mexico 87185

The laminar flowfield and performance of clusters of two-dimensional vertical axis wind turbines are analyzed by idealizing the rotors as momentum sources. The flowfield dominated by the pressure field of the operating turbines is determined by solving the incompressible Navier-Stokes equations and mutual interference is observed to be elliptic in nature. Physical positioning of the turbines with respect to each other significantly affects the aerodynamic performance of the turbines. Several cases are examined starting with one pair of turbines to a cluster as big as 21 turbines. From the two-dimensional cases presented here, it is concluded that downwind turbine performance can be improved by judiciously choosing the angular relative orientation of the turbines. Qualitative analysis of the laminar flowfield is conducted with the help of streamlines and pressure contours. Performance comparisons of the turbines are made with a stand-alone turbine operating under similar flow conditions. This investigation lays the groundwork for the optimization of a wind farm.

Nomenclature

B = number of blades
 C_l, C_d = sectional lift and drag coefficients, respectively
 C_p = power coefficient of the turbine,
 $= (T_o \cdot \omega) / [\frac{1}{2} \rho V_\infty^3 (2RH)]$
 $CPAV$ = average power produced by a turbine in a cluster,
 $= \sum_1^N C_p / N$
 $CPSA$ = power coefficient of a (single) stand-alone turbine in uniform flow
 c = turbine blade chord
 d = turbine spacing (nondimensional radial distance between turbines)
 $\hat{e}_r, \hat{e}_\theta, \hat{e}_z$ = unit vectors in the cylindrical coordinate system r, θ , and z , respectively
 f = resultant aerodynamic force on the blade
 H = turbine height ($H = 1$, for two-dimensional rotors)
 $\hat{i}, \hat{j}, \hat{k}$ = unit vectors in the Cartesian coordinate system X, Y , and Z , respectively
 M = local Mach number
 N = number of turbines in a cluster
 O = center of turbine
 p = static pressure
 R = radius of the turbine
 Re = Reynolds number
 Re_c = Reynolds number based on blade chord and tip velocity, $= (\omega R c \rho) / \mu$
 r, θ, z = cylindrical coordinate system attached to the blade
 S_r, S_θ = time-averaged source terms at a grid point
 s_r, s_θ = time-dependent source terms at a grid point
 S_x, S_y = source terms in the momentum equations (discretized)
 S'_x, S'_y = source terms in the momentum equations (differential)
 T_o = torque generated at the center of the turbine

t = coordinate on the time axis
 u = component of V_{abs} in the x direction
 V_∞ = freestream wind velocity
 v = component of V_{abs} in the y direction
 V_{abs} = absolute velocity of the wind with respect to the inertial system fixed at the center of the turbine
 v_r = component of V_{abs} in the r direction
 v'_r = relative radial velocity of wind observed from the noninertial reference frame fixed to the blades
 V_{rel} = relative velocity of wind observed from the noninertial reference frame fixed to the blades
 v_θ = component of V_{abs} in the θ direction
 v'_θ = relative tangential velocity of wind observed from the noninertial reference frame fixed to the blades
 X, Y, Z = inertial reference frame attached to the center of the turbine O where X is parallel to the freestream wind
 α = blade angle of attack with respect to the relative wind velocity V_{rel}
 $\dot{\alpha}$ = rate of change of angle of attack
 λ = tip-speed ratio, $= (\omega R) / V_\infty$
 ρ = density of air
 μ = viscosity of air
 σ = solidity of the turbine, $= (BC) / (2R)$
 ω = rotational velocity of the turbine

I. Introduction

POWER production by wind turbines is a viable alternative to fossil fuel dependency. An increased acceptance of this fact is evidenced by enormous worldwide research in the last decade. While the Third World countries have the greatest potential for wind power through stand-alone units, the technologically advanced countries consider the wind farm—a cluster of wind turbines at a given location—an attractive means for harnessing wind power on a large scale.

In the United States, California is leading in wind farm activity. It appears that in the absence of the federal energy tax credit laws, only efficient and economically viable wind farms will survive. Therefore, a wind farm owner has to maximize the benefits of his resource—the wind.

Having chosen an energy potential site using wind siting techniques, a wind farm owner's main concern is to optimize the overall performance of the wind farm by determining the turbines' best physical locations. Efficient land use and the wind farm's economy are directly dependent on the mutual spacing and the pattern in which wind turbines are placed.

Presented as Paper 88-2534 at the AIAA 6th Applied Aerodynamics Conference, Williamsburg, VA, June 6-8, 1988; received Sept. 26, 1988; revision received July 24, 1989. Copyright © 1989 by the American Institute of Aeronautics and Astronautics, Inc. All rights reserved.

*Assistant Professor, Computational Fluid Dynamics Center, Department of Aerospace Engineering. Member AIAA.

†Undergraduate Student, Computational Fluid Dynamics Center, Department of Aerospace Engineering. Student Member AIAA.

‡Distinguished Member of Technical Staff.

From an aerodynamic point of view this conclusion arises from two sources: 1) blockage and energy removal effects produced by the wind turbines in the freestream wind, and 2) mutual interference of the turbines and the resulting wake mixing and power degradation along the downwind turbines.

In order to understand these effects better, it is necessary to study the flowfield in and around a wind farm both on a near- and far-wake scale. For this reason an analytical model of a wind farm is presented here.

II. Previous Investigations

The importance of wind turbines in multiple machine arrays has long been recognized, and an extensive amount of research has been conducted. This research can be broadly classified into 1) field tests of full scale turbines, 2) experimental wind-tunnel studies, and 3) analytical model studies.

A. Field Tests

Field tests have increased our basic understanding and statistics of wind turbine performance. Yet, regardless of the number of turbines, field tests have posed difficulties because of terrain effects. The data obtained through different measuring techniques show poor correlation with the observed result.¹ Field tests are also subject to the stochastic nature of wind and changing meteorological situations, making repetition of the observation improbable if not impossible. Besides, because field tests can be conducted only after the wind farm has been constructed, they are of no help in the design stage of the wind farm.

B. Experimental Studies

Extensive wind-tunnel studies have been conducted to analyze the wake of a single turbine,²⁻⁴ as well as two or three turbines.⁵⁻⁸ Using wind simulators (gauze), wind farms with 50 or more machines have also been analyzed.⁹⁻¹¹ These experiments yielded fairly reliable information regarding power production capabilities of the turbine/turbine clusters under investigation. However, wake data and their interpretation have not been very fruitful except to get gross characteristics of the turbine wake.

This failure of the experiments to profile the actual nature of the turbine wakes can be attributed in part to the following reasons:

- 1) Blockage offered by a wind turbine to the flow is not clear and may be beyond the acceptable level for the tunnel cross section.

- 2) Turbulence in the incoming flow seriously affects the results.⁸

- 3) Air speeds in the low-turbulence wind tunnels are not greater than the design wind speed at full scale. This results in model Reynolds numbers being lower than those of the prototype, thus losing dynamic similarity between the model and the full scale. Just how the wake is affected by this difference in Reynolds number is not clear, however.

- 4) In the case of model array studies (using wire gauzes as simulators), geometric similarity is also abandoned owing to the small size of each component in the array⁷; thus, the scaling problem is made even more acute.

All of these reasons reflect the strong dependency on analytical methods of analyzing wind turbine interference until such time as a low-turbulence variable-density facility is available for properly simulating dynamically similar turbine flow.

C. Analytical Model Studies

Several methods have been used to study the overall performance and characteristics of stand-alone vertical axis wind turbines. A brief and essential comparison of the important methods is given in Ref. 12. The discussion here will be restricted to methods used for wind turbine array modeling only.

1. Boundary-Layer Theories

Analytical modeling of arrays using the planetary, boundary-layer concept was first initiated by Templin¹³ with the objective of obtaining the overall power output of large arrays. Subsequently, Crafoord,¹⁴ Newman,¹⁵ Bragg and Schmidt,¹⁶ Taylor,¹⁷ and Best¹⁸ modified this approach with varying degrees of approximations and successfully predicted the overall performance of the arrays.

The boundary-layer approach is a macroscopic approach in which the drag-generating wind turbines are considered as uniformly smeared roughness elements inside the boundary layer. As a consequence, an individual turbine's geometric and dynamic characteristics and the mutual interference of turbines are neglected. More recently, Liu et al.¹⁹ have improved the boundary-layer approach using hydrostatic approximation to the three-dimensional boundary-layer equation, wherein they have considered the individual turbine's characteristics via actuator disk theory and axial interference factors. However, they have considered the velocity defect in the axial direction only.

Boundary-layer approximation of the flow through a wind turbine treats the flow as parabolic in at least one coordinate direction, while the actual flow is elliptic in all three coordinate directions. Although this approximation is justifiable for evaluation of macroscopic properties such as overall power output of the array of turbines, the approach as such does not shed light on the wake interacting region between the wind turbines. This is mainly because the wake region of a wind turbine cluster is characterized by the strong mutual (elliptic) interference induced by the operation of rotors and the turbulent viscous interchange of momentum between the wake and the main stream flow, in addition to other reasons such as the presence of the pressure gradient in the flowfield.

2. Wake Superposition Theories

This approach, initially proposed by Lissaman,²⁰ was derived from jet-mixing theories. Existing wake decay data of circular jets immersed in a uniform flow were correlated to wind turbine wakes to model the interacting wakes of wind turbines. The fundamental assumptions in this technique are that the velocity profiles in the wake region are self-similar and that the velocity incident on successive rows in an array would decay progressively, leading to similar power decay. Also, the wake radius of one turbine assumed to grow in a geometric fashion is linearly superposed to model the interacting wakes of the array of turbines. Sforza²¹ and Vermeulen²² subsequently improved this method by using semiempirical descriptions of the flowfield of a single turbine's wake (based on experiments) instead of the original data from circular jets immersed in uniform flow.

The real interaction between wind turbines is more complex than linear addition of wakes would permit. Also, linear superposition of velocity defects restrains the momentum deficit in the turbine wake (because of the extraction of power by a wind turbine) to be conserved, whereas the real flowfield is complicated by the viscous momentum diffusion between the wake and the outer main flow. Although this approach recognizes individual turbines, it has limitations as far as the near-wake region modeling is concerned. For wake interaction studies, this technique has been discouraging as reported by Alfredsson et al.⁸

3. Momentum Theories

A different approach is taken by Pershing²³ to analyze the slipstream interference between windmills in a closely spaced array by taking into consideration the stream tube interference of the upwind rotor on the downwind rotor based on classical actuator disk theory. A similar approach is taken by Loth and McCoy²⁴ to determine the performance limit of infinite actuators in series.

In momentum theories it is assumed that the wake of a turbine is fully developed before it interferes with the down-

wind rotor; thus, no upstream influence is considered. Since the momentum theories are basically one-dimensional approaches developed to give first-cut information about the overall limiting performance, they are not suitable for wake interference analysis.

Before proceeding to the next theory, it is important to note here that the aforementioned array performance theories either did not consider the individual characteristics of the turbines or treated them as those of horizontal axis wind turbines idealized as actuator disks. This brings us to the next theory, the free-vortex approach, which is the only theory that can analyze the mutual interference of two vertical axis wind turbines with prediction capabilities for both near and far wake.

4. Free-Vortex Theories

The free-vortex wake models initiated by Fanucci and Walters²⁵ and improved by Strickland et al.³ are very accurate and suitable for wake prediction of vertical axis wind turbines. The only aerodynamic model that analyzed the interference of two Darrieus-type wind turbines is the work of Schatzle et al.²⁶ They used the vortex/lifting line theory of Strickland et al.³ and investigated the detailed wake structure of two Darrieus wind turbines with a tower-to-tower separation distance of 1.5 rotor diameters. The model was very accurate in that it considered the mutual interference of three-dimensional turbines in contrast to all previous research. Their research concluded that the downwind turbine power decrement is a strong (directly proportional) function of the tip-speed ratio and induced flow angularities and not so strong a function of the velocity defect itself when the line of turbine centers was not coincident with the ambient wind direction.

The model, however, had some limitations: 1) It required that the tower-to-tower separation distances be small to obtain meaningful results, and 2) the computer run times were prohibitively high.

D. Summary of Previous Analytical Investigations

Boundary-layer models use a macroscopic approach and are useful for predicting the overall power output of a turbine cluster. However, boundary-layer approximation treats the flow as parabolic in at least one coordinate direction, whereas the flow through the wind turbine is elliptic in all directions. In general, the individual turbine characteristics are not considered. When they are, only the horizontal axis wind turbines with axial momentum defect are considered. The angular momentum induced is neglected in the analysis.

Wake superposition theories assume that the wakes of individual turbines are linearly superposable for modeling the wake interaction. This distorts the true elliptic nature of the flow through a wind turbine cluster due to neglect of mutual interference.

Because momentum theories were one-dimensional in nature, their very purpose was to determine the gross overall power output of the turbine array, which they did well. They are not, however, suitable for wake prediction of turbines and certainly not wake interference.

Free-vortex theory has been successful but is limited in scope to situations of small tower-to-tower distances and hence is not suitable for tower-to-tower distance optimization and wind farm study. Besides, the computational cost has been prohibitively high.

Thus, most of the analytical models discussed so far served their intended purpose very well, that is, an overall assessment of the gross power production potential of an array of turbines. As far as individual characteristics are concerned, as discussed previously, they all had their advantages and deficiencies. Among the deficiencies, mutual interference of wind turbines in a cluster was not considered in detail, and no qualitative measure of the interference was established. This research attempts to fill in this deficiency by comparing individual turbine performance as a stand-alone and in a cluster.

III. Aerodynamic Model

Rajagopalan and Fanucci¹² developed a finite-difference model using computational fluid dynamics for representing the action of a single two-dimensional Darrieus turbine in inviscid, incompressible flow. In this formulation, the spinning blades are idealized as point momentum sources thereby avoiding the computation of blade flow. The technique has been further extended to laminar flowfield by Rajagopalan.²⁷ In their analysis the flowfield is assumed to be steady. Their investigations illustrated that while the true flowfield of a Darrieus rotor is unsteady, a time-averaged solution represents the flowfield in sufficient detail once a steady-state rotational velocity is reached by the rotor blades. For the present study, the same framework is used with necessary modifications to include multiple turbines. Since the steady incompressible Navier-Stokes equations are elliptic in nature, this method is suitable for aerodynamic interference study. In addition, the computational cost of calculating the flowfield and performance of the turbines using this procedure, as it is presented here, depends mainly on the number of finite-difference grid points and is only a very weak function of the number of turbines.

The modeling of the laminar flowfield of the turbine cluster can be conveniently considered under two separate subheadings, namely, the flowfield modeling and the aerodynamic modeling of turbines.

A. Flowfield Modeling

The numerical procedure is based on Patankar's "SIMPLER" algorithm.²⁸ After assuming that the flowfield is steady, the laminar, incompressible, Navier-Stokes equations governing the two-dimensional array of turbines placed in a Cartesian coordinate system are

Mass:

$$\frac{\partial u}{\partial x} + \frac{\partial v}{\partial y} = 0 \quad (1)$$

x momentum:

$$\rho \left(u \frac{\partial u}{\partial x} + v \frac{\partial u}{\partial y} \right) = \mu \left(\frac{\partial^2 u}{\partial x^2} + \frac{\partial^2 u}{\partial y^2} \right) - \frac{\partial p}{\partial x} + S'_x \quad (2)$$

y momentum:

$$\rho \left(u \frac{\partial v}{\partial x} + v \frac{\partial v}{\partial y} \right) = \mu \left(\frac{\partial^2 v}{\partial x^2} + \frac{\partial^2 v}{\partial y^2} \right) - \frac{\partial p}{\partial y} + S'_y \quad (3)$$

where *u* is the *i* component of velocity, *v* is the *j* component of velocity, *p* is the static pressure, μ is the flow viscosity, and S'_x and S'_y are the time-averaged source terms per unit cell volume around a grid point due to the turbines to be discussed next. Even though turbulence plays an important role in turbine performance, only laminar flow is considered in this initial analysis.

The conservation of mass and momentum equations (the Navier-Stokes equations) are solved using a finite-difference approach. The Cartesian computational domain is subdivided into control volumes by a series of grid lines orthogonal to the *i* and *j* coordinate directions. The size of the control volumes is decided based on the accuracy required in the region. Accordingly, the wake and the immediate vicinity of the turbines have a very fine mesh.

The flowfield is determined by solving for the primitive variables *p*, *u*, and *V* directly from the mass and momentum conservation equations. These flow equations, written in conservation form, are discretized using a control volume approach, and the resulting elliptic equations are solved by a line-by-line method combining the tridiagonal matrix algorithm and the Gauss-Seidel method. Upwind differencing is

used for interpolating the variables u and v at the control volume faces. Details of the method are found in Ref. 28.

B. Aerodynamic Modeling of Turbines

The vertical axis wind turbine blades as they revolve, in addition to other things, deflect and decelerate and/or accelerate the flow. In other words, they primarily change the vector momentum of the fluid. The local momentum of the fluid is changed due to the forces generated by the rotating blades. Thus, a logical place to incorporate the action of the blades in the governing equations of the fluid flow is through the source terms of the momentum equations, namely, S'_x and S'_y or through their counterpart S'_x and S'_y (the integrated form of S'_x and S'_y) the source terms in the momentum equations. For a time-accurate calculation, the source terms in functional notation can be written as

$$S_x = S_x(C_l, C_d, \alpha, \dot{\alpha}, V_{abs}, \omega, R, \theta, t, c, \rho, \mu, Re, M, B)$$

$$S_y = S_y(C_l, C_d, \alpha, \dot{\alpha}, V_{abs}, \omega, R, \theta, t, c, \rho, \mu, Re, M, B)$$

where C_l and C_d are airfoil characteristics of the turbine blade, α is the angle of attack made by the turbine blade to the relative velocity vector, $\dot{\alpha}$ is the time rate of change of α as the blade moves through a revolution, V_{abs} is the absolute velocity of the fluid at the instantaneous blade location (R, θ, t) , ω is the angular velocity of the rotor, c is the chord of the blade, and B is the number of blades.

Since the operational regime of a vertical axis wind turbine is well within the acceptable range of Mach numbers for incompressible flow, S_x and S_y are not considered functions of M , the local Mach number of the flow. Even though the complete Navier-Stokes equations are solved everywhere in the flowfield, the dependence of S_x and S_y on μ and Re are considered only implicitly through the airfoil sectional characteristics C_l and C_d in this analysis. The influence of α is of importance when dynamic stall is considered but is neglected for this investigation. However, these are not restrictions and can be included in the analysis where they are considered important. Thus, the source terms after time averaging reduce to

$$S_x = S_x(C_l, C_d, \alpha, V_{abs}, \omega, R, \theta, t, c, \rho, B)$$

$$S_y = S_y(C_l, C_d, \alpha, V_{abs}, \omega, R, \theta, t, c, \rho, B)$$

The true flowfield of a vertical axis wind turbine is unsymmetrical and unsteady. However, a time-averaged solution represents the flowfield in sufficient detail and yields accurate performance characteristics. Accordingly, S_x and S_y used in this analysis are time-averaged momentum sources due to the motion of the turbine blades.

Following a procedure illustrated in Ref. 12, and with the help of Fig. 1, forces due to lift and drag in the blade-fixed r and θ directions, respectively, are

$$s_r = (c \times 1)(\rho V_{rel}^2/2)(C_l \cos \alpha + C_d \sin \alpha) \quad (4)$$

$$s_\theta = (c \times 1)(\rho V_{rel}^2/2)(C_l \sin \alpha + C_d \cos \alpha) \quad (5)$$

where $c \times 1$ is the area of unit span of blade and $\rho V_{rel}^2/2$ is the dynamic pressure seen by the blades.

From the velocity diagram in Fig. 1 it can be seen that

$$v'_r = V_{rel} \sin \alpha \quad (6)$$

$$v'_\theta = -V_{rel} \cos \alpha \quad (7)$$

where v'_r and v'_θ are the relative velocity components seen by the blade-fixed (r, θ) coordinate system. Using the relations in Eqs. (6) and (7), angle of attack α is eliminated from the force

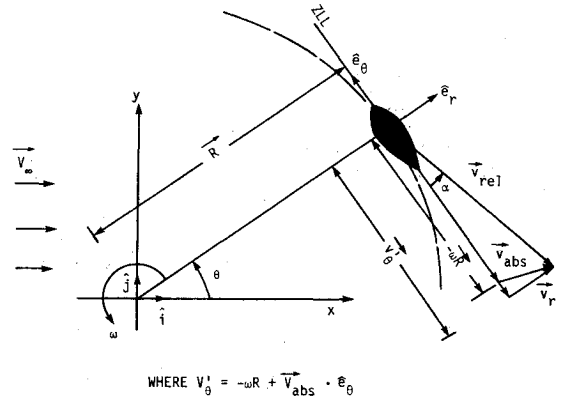


Fig. 1 Coordinate systems and velocity vectors.

equations, Eqs. (4) and (5), to yield

$$s_r = c(\rho V_{rel}/2)(-C_l v'_\theta + C_d v'_r) \quad (8)$$

$$s_\theta = c(\rho V_{rel}/2)(C_l v'_r + C_d v'_\theta) \quad (9)$$

Each blade of a turbine passes through a series of grid points, and associated with each one is a control volume. As the blade goes through a complete revolution, its path makes a full circle or 2π radians in angular measure. Thus, if $R\Delta\theta$ is the arc length intersected by a specific control volume associated with a grid point, then $(\Delta\theta/2\pi)$ is the fraction of the time spent by the blade within this control volume in one given revolution. If there are B number of blades in a turbine, then the fraction of the time spent by all the blades collectively within a control volume will be equal to $(B\Delta\theta/2\pi)$. Thus, multiplying Eqs. (8) and (9) by this fraction gives the time-averaged forces in the blade-fixed r and θ directions, respectively, as

$$S_r = (c\rho V_{rel}/2)(B\Delta\theta/2\pi)(-C_l v'_\theta + C_d v'_r) \quad (10)$$

$$S_\theta = (c\rho V_{rel}/2)(B\Delta\theta/2\pi)(C_l v'_r + C_d v'_\theta) \quad (11)$$

Resolving these forces in the inertial coordinate directions x and y , respectively, using the relation

$$S_x = S_r \cos \theta - S_\theta \sin \theta \quad (12)$$

$$S_y = S_r \sin \theta + S_\theta \cos \theta \quad (13)$$

yields the required momentum sources to be subtracted at a grid point.

Each turbine in the cluster has associated with it a circle denoting its blade path and a series of grid points along the circles. The source terms S_x and S_y are evaluated at all of these grid points, and they are grid specific. They are evaluated for each iteration until there is a mass and momentum balance in the entire flowfield. The relative velocity components v'_r and v'_θ are evaluated from the relations

$$v'_r = V_{abs} \cdot \hat{e}_r$$

$$v'_\theta = V_{abs} \cdot \hat{e}_\theta - \omega R$$

The sectional aerodynamic coefficients are evaluated as a function of local Reynolds number based on V_{rel} and section chord from a table containing a complete variation of C_l vs α and C_d vs α for the entire range of $\alpha = 0-360$ deg. Thus, this procedure allows for the turbines to be aerodynamically and geometrically different in characteristics while operating at different rotational speeds with complete freedom in the choice of their location in the flowfield. Since the governing

partial differential equations are elliptic and the discretized equations are solved simultaneously, mutual aerodynamic interference of the turbines is considered completely.

In closing, it is important to mention that although the present method considers the geometric characteristics of the turbine blades for the evaluation of the point momentum sources that represent the action of the turbine blades, the actual geometry of the blades does not affect the flow directly through the conventional no-slip body boundary condition. In other words, blade boundary layer is not computed as part of the solution.

IV. Results

The specific objectives of this research are to determine computationally 1) the extent of mutual interference of vertical axis wind turbines placed in a uniform upstream flow, 2) if there are any angular relative orientations of the turbines that maximize the power production of the turbines, and 3) if the conclusions of the preceding two items can be used advantageously in arranging larger clusters of turbines. To this end, several specific exercises were conducted and their results are reported here.

The computational setup has freedom to vary all aerodynamic and geometric characteristics of the turbines collectively as well as individually in a manner suitable for parametric optimization. However, for all cases reported here the turbines were assumed to have the same geometric and aerodynamic characteristics. All of the turbines were two-bladed and have a four-unit diameter with a solidity ($Bc/2R$) of 0.075. NACA0015 was used for blade sectional characteristics and the table look-up for $\alpha = 0-360$ deg was interpolated for local Reynolds number based on V_{rel} and c . However, the local Reynolds number based on the relative velocity seen by the blades varies as a function of the azimuthal position given by θ . Hence, a fixed Reynolds number based on the linear rotational velocity of the blade tip (ωR) and the blade chord c , namely, $Re_c = \omega R c \rho / \mu$ (chosen to be 1.5×10^6), was used for identifying the operational conditions in the figure legends.

A fine mesh was used in the immediate vicinity of the turbines such that on the average there are about 30 grid points in the blade path of every turbine. All force and power computations are integrated for these grid points. If f is the resultant aerodynamic force felt by the blades, then

$$f = s_r \hat{e}_r + s_\theta \hat{e}_\theta$$

$$T_o = \sum R \times f$$

$$C_p = \{T_o \cdot \omega / [\frac{1}{2} \rho V_\infty^3 (2RH)]\}$$

where the summation is taken over all the grid points mentioned earlier.

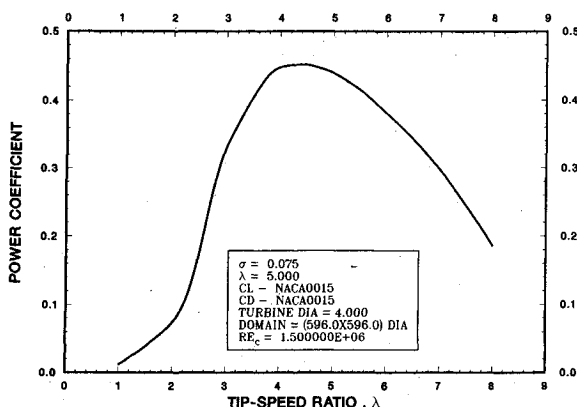


Fig. 2 Performance of stand-alone turbine.

The power coefficient C_p of a stand-alone turbine was computed for several tip-speed ratios ($\lambda = \omega R / V_\infty$) on a 150×150 grid covering a physical region of 596×596 diam. Both the physical size and the computational grid structure were chosen from knowledge gained in previous research.²⁹ From the C_p vs λ variation given in Fig. 2, a tip-speed ratio of 5, based on the peak power production, was chosen as the rotational speed of all of the turbines in clusters discussed here. The number of grid points and the physical computational domain were chosen to be adequate for larger clusters and is maintained for all cases including a stand-alone turbine reported here for reasons of comparison.

The first cluster to be considered is the simple case of a pair of identical turbines operating at a tip speed $\lambda = 5$. The blade path is seen as two circles in Fig. 3. The rim-to-rim distance along the line connecting the centers d and the angle θ made by this line to the freestream wind in the direction of the Cartesian x axis are varied. The turbines are numbered using matrix notation representing row-column elements. Accordingly, the two turbine cluster turbines are named 11 and 12. Figure 4 compares the performance of the two turbines for a distance $d = 6$ turbine diameters for several angles. When the angle is 0 deg, the two turbines are aligned with the freestream, and turbine 12 is completely in the wake of turbine 11. For the two-dimensional situation studied here, the power output of turbine 12 is significantly low when $\theta = 0$ deg. In other words, if two turbines are placed one behind the other in line with the freestream wind and are forced to operate at a given rotational velocity as is done in this analysis, the second turbine requires power to operate rather than being able to extract power from the wind.

It is well known that wake overlap adversely affects the performance of the downwind turbine. However, the ill ef-

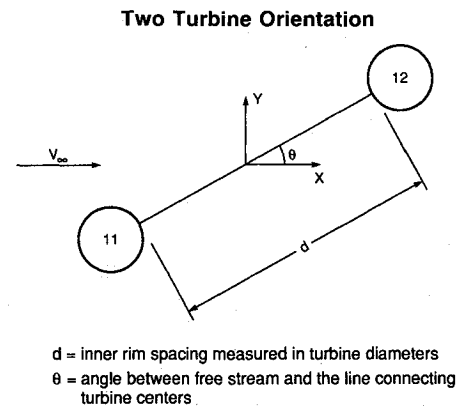


Fig. 3 Turbine cluster nomenclature.

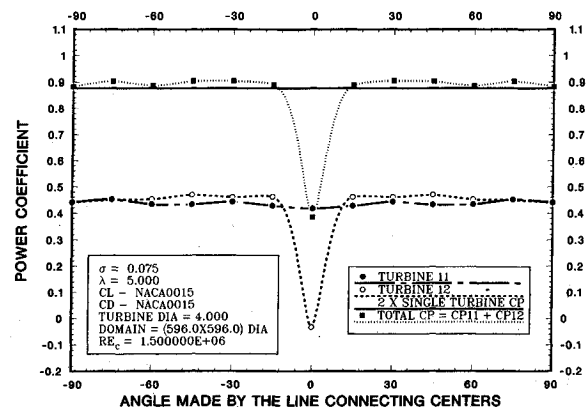


Fig. 4 Power coefficient for two turbines with spacing = 6.00.

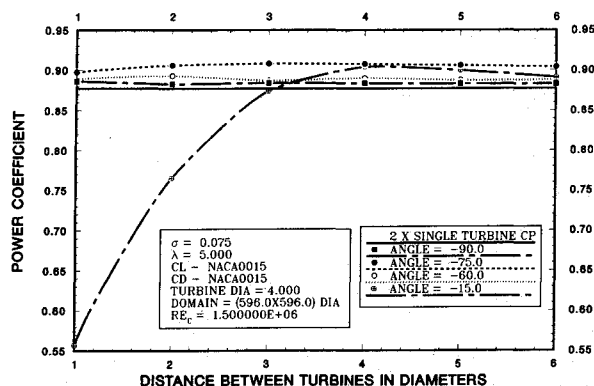


Fig. 5 Combined power coefficient for increasing turbine spacing.

fects of the interference is not limited to the downwind turbine alone. As is seen in Fig. 4, the lowest level of power production for both the turbines is when there is any overlap and is in the range of -6 to 6 deg for this specific example. Compared to the nondimensional power produced by a single stand-alone turbine = 0.4388, both the turbines in the cluster produce more power outside of the wake overlap angles for this separation distance. Also, in this non-wake-overlap region, due to the mutual aerodynamic interference and the induced flow angularity, the downwind turbine produces slightly more power than the upstream turbine. It is observed that the nature of the curve is roughly symmetric, about $\theta = 0$ deg. In the same figure, the total output of both the mutually interacting turbines is compared with that of twice the power output of a single stand-alone turbine operating under the same conditions. Except for a narrow range of θ around $\theta = 0$ deg the overall power output of the mutually interacting turbines is greater. When no wake overlap is present, two turbines operating under certain preferred angular orientations could output a net power higher than the combined output of two stand-alone turbines; this is further confirmed in Fig. 5 where the nondimensional distance between the two turbines is varied from 1 through 6 for certain angles and the results are cross plotted. The angular orientation range of -90 to -60 deg (or the symmetric range of 60 – 90 deg) appears to be the most favorable range where the combined power coefficient for the two turbine cluster system is more than twice the single turbine power coefficient. It is to be noted here that these results generally show a trend that two turbines operating under certain favorable angular orientations, outside of wake overlap regions, produce more combined power than two independent turbines. Exactly what orientation range is best depends on all the characteristics of the turbines such as the radius, the rotational velocity, the airfoils used for the blades, etc. Thus, the qualitative results may vary significantly for turbines with different characteristics.

Three cases of four turbine clusters are analyzed next. A turbine spacing of 1 diam between any two adjacent turbines is used henceforth. Figures 6a–6c describe the angular orientation of the turbine rows, 0, 60, and -90 deg, respectively, and the streamline pattern of the flow around them. The legends give the characteristics of the turbines and the power coefficient C_p of the individual turbines. The average C_p of the turbines is denoted by $CPAV$ and the stand-alone unit power is given by $CPSA$. In Fig. 6a, the downwind turbines (12 and 22) are completely in the wake of the upwind turbines (11 and 21). The downwind turbines produce significantly lower power, and all the turbines produce lower power than a stand-alone turbine, thereby showing that unfavorable mutual interference not only affects the downwind turbine but also deteriorates the upwind turbine performance. The situation dramatically improves in Fig. 6b where the turbine rows make 60 deg to the freestream. The $CPAV$ is higher than $CPSA$ and

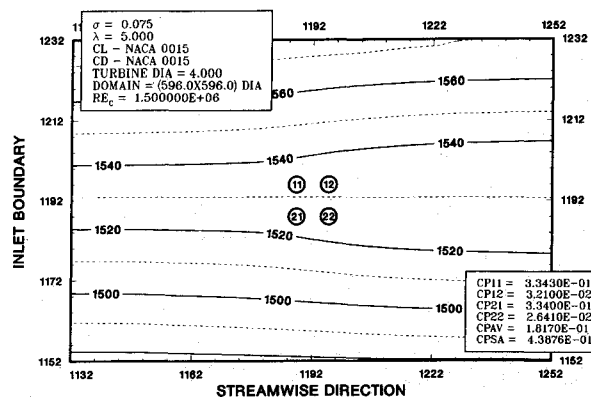


Fig. 6a Streamlines through a four-turbine cluster: 0-deg rows.

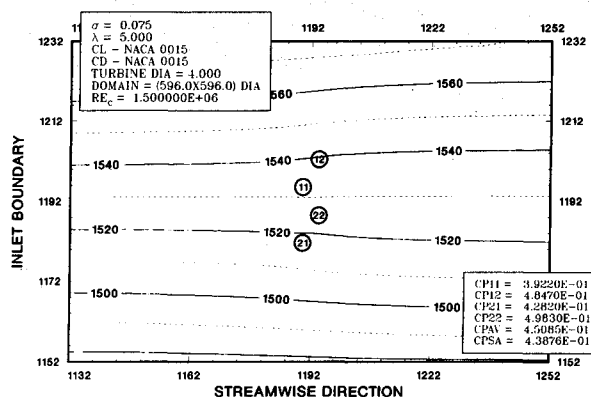


Fig. 6b Streamlines through a four-turbine cluster: 60-deg rows.

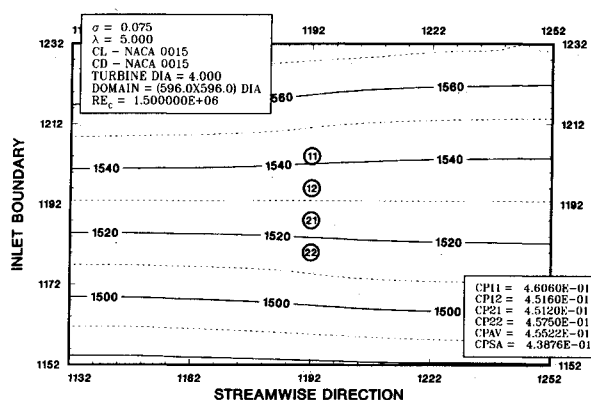


Fig. 6c Streamlines through a four-turbine cluster: -90 -deg rows.

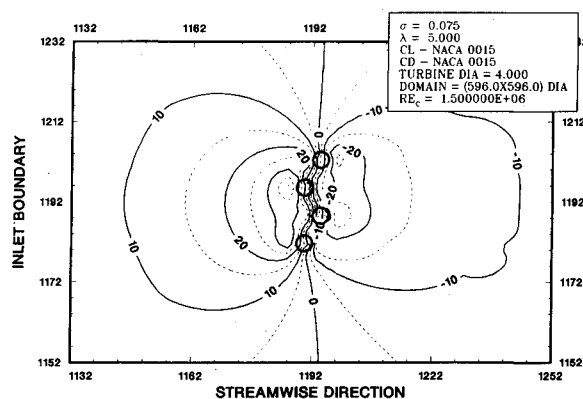


Fig. 6d Pressure contours in a four-turbine cluster flowfield: 60-deg rows.

the upwind turbines 11 and 21, under the influence of the downwind turbines 12 and 22, have lower power output than *CPSA*. This further substantiates the earlier finding that certain preferred orientations may actually enhance the power production potential of the downwind turbines and the overall performance of the cluster. Also noteworthy is that the turbine 21, which has only one downwind turbine 22 to influence it, has a higher C_p than turbine 11. In contrast, turbine 22 produces more power, in part attributable to the stream-tube contraction forced by turbines 11 and 21 and the associated higher incoming flow velocity. Thus, from an overall standpoint it appears that the turbines that are in the front row (turbines 11 and 21) facing the undisturbed incoming wind generally produce less power in the cluster. In Fig. 6c the turbine rows make -90 deg to the horizontal. The *CPAV* is the highest in this case, and the individual turbine C_p of any turbine in the cluster is higher than *CPSA*. This clearly shows that the interference between the turbines is strongly elliptic.

The incompressible flow through the turbines is dominated by the pressure field. In Fig. 6d, contours of pressure for the case of $\theta = 60$ deg (corresponding to the configuration in Fig. 6b) is given. A strong interaction between the turbines is seen. Most important are the positive static pressure contours seen in front of the turbine cluster, denoting the lower flow velocity entering the turbine. As the levels of positive contours increase in front of a turbine, less and less power is available in the flow for that turbine to extract. This is validated by the lower power produced by turbine 11, as shown in Fig. 6b.

From the experience gained in two and four turbine clusters, larger arrays were arranged. For reasons of land economy, the angular orientation of the turbine rows was maintained at the lower angle of 60 deg from the favorable θ range. Nine tur-

bines are arranged in two patterns in Figs. 7a and 7b. In these two patterns, no turbine path is directly behind any upwind turbine path. The turbines at the beginning of rows generally produce lower power, and the turbines at the end of rows produce more power. Turbine 21 in Fig. 7b is placed in such a way that it sees the wind flowing through turbines 11 and 31. The stream tubes narrow in this region, suggesting an increase in velocity, and this is substantiated by the higher power produced by turbine 21 that experiences this increased flow velocity. A similar behavior is seen for turbines 23 and 33 in Fig. 7a.

Figures 8a and 8b portray two different 21 turbine clusters. Unlike the configurations in Fig. 7, turbines are placed to operate directly behind upwind turbines. Accordingly, turbine 45 is directly behind turbine 22 in Fig. 8a. As was observed in earlier cases, upwind turbines initially facing the undisturbed stream have generally lower power output, validating the earlier finding that there is strong mutual interference between the upwind and downwind turbines. Even though a turbine is completely immersed in the wake of another turbine, in larger clusters like this they produce more power than if there are only two turbines in the cluster with one being placed directly behind the other ($\theta = 0$ deg case discussed earlier with regard to Fig. 4). For example, turbine 45 directly behind turbine 22 produces significantly more power ($CP_{45} = 0.1192$) than turbine 12 ($CP_{12} = 0.0321$) or turbine 22 ($CP_{22} = 0.02641$) in a four-turbine cluster in Fig. 6a as well as turbine 12 for $\theta = 0$ deg ($C_p_{12} < 0$) in a two-turbine cluster in Fig. 4. A similar behavior is exhibited in Fig. 8b. A possible reason for this phenomenon can be traced to the large wake mixing that exists in larger clusters.

Finally, the computation times for the turbines are com-

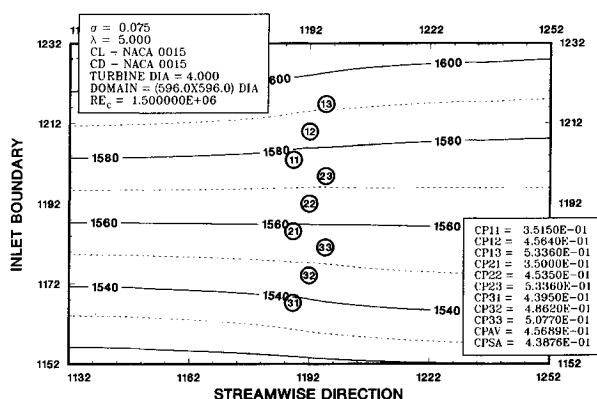


Fig. 7a Streamlines through a nine-turbine cluster (slant-type): 60-deg rows.

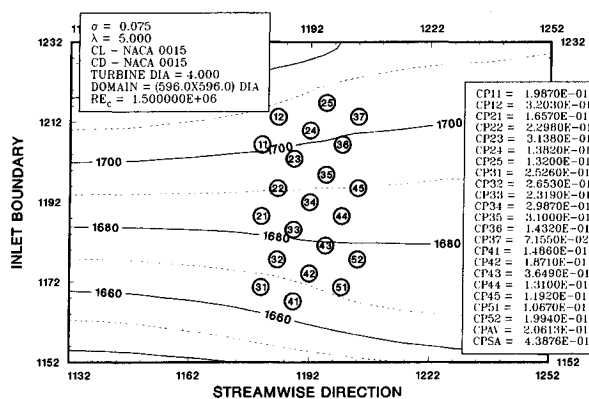


Fig. 8a Streamlines through a 21-turbine cluster (slant-type): 60-deg rows.

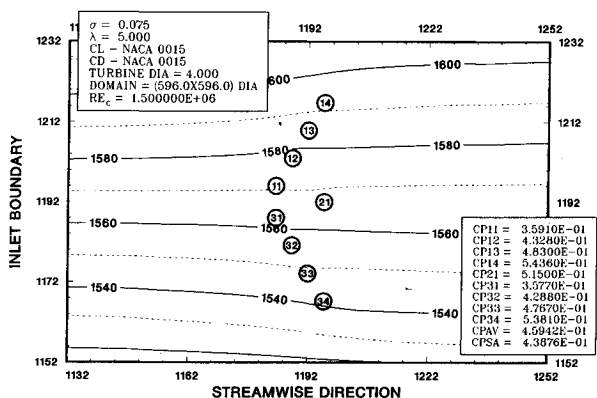


Fig. 7b Streamlines through a nine-turbine cluster (V-type): 60-, 0-, and -60-deg rows.

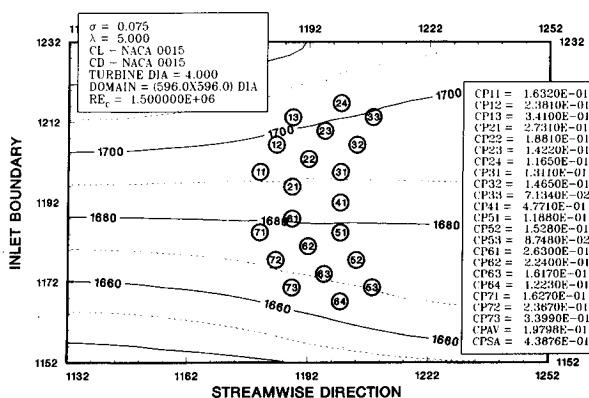


Fig. 8b Streamlines through a 21-turbine cluster (V-type): 60-, 0-, and -60-deg rows.

Table 1

Number of turbines in the flowfield	CPU times, s
1	595
4	603
9	612
21	640

pared in Table 1 for the same number of grid points (150×150) on the computer system NAS9160. The computations done for a turbine are independent of the number of turbines in the cluster and the CPU times given in the table strongly indicate that the computation times are only a very weak function of the number of turbines in a flowfield.

Table 1 gives typical computation time for a converged flowfield solution after 250 iterations of a given.

V. Conclusions

Using computational fluid dynamic techniques, the laminar flowfield of clusters of two-dimensional turbines is analyzed. In this approach, since it uses an elliptic algorithm for solving the fluid flow equations, interference of turbines is captured completely. The individual turbines are represented by momentum sources that functionally account for a complete description of geometric and aerodynamic characteristics.

Specific conclusions directly related to the results are the following:

- 1) Mutual interference is strong and dominates the performance of wind turbine clusters.
- 2) A certain angular range closest to the line connecting the centers being vertical (facing the wind perpendicularly) is very favorable for improved performance.
- 3) Downwind turbines arranged along rows of favorable angle with no overlap show better performances than a turbine placed first in the row facing an undisturbed stream.
- 4) The performance of turbines operating completely in the wake of other turbines can be improved by judiciously choosing their position such that they see a higher flow velocity due to the presence of other turbines and associated stream-tube contraction.
- 5) The average performance of turbines in advantageously positioned arrays may be better than the performance of stand-alone turbines.
- 6) The method is robust and computationally economical and is an efficient technique for array performance and wake analysis.

The research also points out that there is a lot of scope for future research:

- 1) Two-dimensional analysis may not account for all of the three-dimensional pressure relieving effects known in flows around three-dimensional bodies. Currently, research is under way to develop a three-dimensional model capable of performing array performance studies in a three-dimensional elliptic flowfield.
- 2) Turbulence plays an important role in wind turbine performance and may be an important factor in the estimation of array performance. This procedure allows for studying the effect of turbulence in detail, properly accounting for all turbulence production due to the action of the turbines.
- 3) Array performance needs to be studied using multivariable parametric optimization techniques while properly accounting for mutual aerodynamic interference.

Acknowledgments

The work was carried out under the support of the Engineering Research Institute of Iowa State University and Sandia National Laboratories. All of the computing for this project was provided by the Iowa State Computation Center as part of a block grant.

References

- ¹Gordon, L. H., "Mode-2 Wind Turbine Field Operations Experience," *Proceedings of the 19th IECEC*, American Nuclear Society, San Francisco, CA, Paper No. 849424, Aug. 1984, pp. 2363-2368.
- ²Blackwell, B. F., Sheldahl, R. E., and Feltz, L. V., "Wind Tunnel Performance Data for the Darrieus Turbine with NACA 0012 Blades," Sandia National Laboratories, Albuquerque, NM, Rept. SAND 76-0130, May 1976.
- ³Strickland, J. H., Webster, B. T., and Nguyen, T., "A Vortex Model of the Darrieus Turbine: An Analytical and Experimental Study," *Journal of Fluids Engineering*, Vol. 101, Dec. 1979, pp. 500-505.
- ⁴Builtjes, P. J. H., and Smit, J., "Calculation of Wake Effects in Wind Turbine Parks," *Wind Engineering*, Vol. 2, No. 3, 1978, pp. 135-145.
- ⁵Ljungstrom, O., "Large Scale Wind Energy Conversion System (WECS) Design and Installation as Affected by Site Wind Energy Characteristics, Grouping Arrangement and Social Acceptance," *Wind Engineering*, Vol. 1, No. 1, 1977, pp. 36-57.
- ⁶Milborrow, D. J., "The Performance of Arrays of Wind Turbines," *Journal of Industrial Aerodynamics*, Vol. 5, 1980, pp. 403-430.
- ⁷Clayton, B. R., and Filby, P., "Wind Turbine Wake Studies," *Proceedings of the Third BWEA Wind Energy Conference*, BHRA Fluid Engineering, Cranfield, April 1981, pp. 172-184.
- ⁸Alfredsson, P. H., Dahlberg, J. A., and Vermeulen, P. E. J., "A Comparison between Predicted and Measured Data from Wind Turbine Wakes," *Wind Engineering*, Vol. 6, No. 3, 1982, pp. 149-155.
- ⁹Milborrow, D. J., "Measurement and Interpretation of Wind Turbine Wake Data," *Proceedings of the Third BWEA Wind Energy Conference*, BHRA Fluid Engineering, Cranfield, April 1981, pp. 153-164.
- ¹⁰Metherell, A. J. F., Sawyer, A., Wilson, D. M. A., Milborrow, D. J., and Ross, J. N., "Wind Tunnel Studies of Interacting Wind Turbines," *Proceedings of the 4th BWEA Wind Energy Conference*, BHRA Fluid Engineering, Cranfield, March 24-26, 1982, pp. 237-247.
- ¹¹Ross, J. N., and Ainshie, J. F., "Wake Measurements in Clusters of Model Wind Turbines Using Laser Doppler Anemometry," *Proceedings of the 4th BWEA Wind Energy Conference*, BHRA Fluid Engineering, Cranfield, 1982.
- ¹²Rajagopalan, R. G., and Fanucci, J. B., "Finite Difference Model for Vertical Axis Wind Turbines," *Journal of Propulsion and Power*, Vol. 1, No. 6, 1985, pp. 432-436.
- ¹³Templin, J., "An Estimate of the Interaction of Windmills in Widespread Theory Arrays," National Research Council, Ottawa, Ontario, Canada, LTR-LA-171, 1974.
- ¹⁴Crafoord, C., "An Estimate of the Interaction of a Limited Array Theory of Windmills," Dept. of Meteorological Institute, Stockholm, Sweden, DM-16, 1975.
- ¹⁵Newman, B. G., "The Spacing of Wind Turbines in Large Arrays," *Energy Conversion*, Vol. 16, 1977, pp. 169-171.
- ¹⁶Bragg, G. M., and Schmidt, W. L., "Determination of Optimum Arrays Theory of Wind Energy Conversion Devices," *Journal of Energy*, Vol. 2, No. 3, May-June 1978, pp. 155-159.
- ¹⁷Taylor, P. A., "Power Reduction in Wind Farm Arrays—An Application to the Array Proposed for the Kahuku Hills," *Wind Engineering*, Vol. 4, No. 2, 1980.
- ¹⁸Best, R. V. B., "The Capacity Factor of a Wind Turbine Cluster," *Wind Engineering*, Vol. 5, No. 4, 1981, pp. 235-241.
- ¹⁹Liu, M.-K., Yocke, M. A., and Myers, T. C., "Mathematical Model for the Analysis of Wind-Turbine Wakes," *Journal of Energy*, Vol. 7, No. 1, Jan.-Feb. 1983, pp. 73-78.
- ²⁰Lissaman, P. B. S., "Energy Effectiveness of Arbitrary Arrays of Wind Turbines," *Journal of Energy*, Vol. 3, Nov.-Dec. 1979, pp. 323-328.
- ²¹Sforza, P. M., "Wind Turbine Generator Wakes," AIAA Paper 79-0113, Jan. 1979.
- ²²Vermeulen, P. E. J., "An Experimental Analysis of Wind Turbine Wakes," *Proceedings of the 3rd International Symposium on Wind Energy Systems*, Copenhagen, BHRA, Cranfield, 1980.
- ²³Pershing, B. M., "Performance Theory of Windmills in a Closely Spaced Array," *Journal of Energy*, Vol. 3, No. 3, May-June 1979, pp. 185-187.
- ²⁴Loth, J. L., and McCoy, H., "Optimization of Darrieus Turbines with an Upwind and Downwind Momentum Model," *Journal of Energy*, Vol. 7, No. 4, July-Aug. 1983, pp. 313-318.
- ²⁵Fanucci, J. B., and Walters, R. E., "Innovative Wind Machines: The Theoretical Performance of a Vertical Axis Wind Turbine,"

Proceedings of the Vertical Axis Wind Turbine Technology Workshop, Sandia National Lab., Albuquerque, NM, SAND 76-5586, Paper III, May 1976.

²⁶Schatzle, P. R., Klimas, P. C., and Spahr, H. R., "Aerodynamic Interference Between Two Darrieus Wind Turbines," *Journal of Energy*, Vol. 5, No. 2, March-April 1981, pp. 84-88.

²⁷Rajagopalan, R. G., "Viscous Flow Field: Analysis of a Vertical Axis Wind Turbine," *Proceedings of the 21st Intersociety Energy Conversion Engineering Conference*, Vol. 2, San Diego, California, Aug. 25-29, 1986, Paper 869275.

²⁸Patankar, S. V., *Numerical Heat Transfer and Fluid Flow*, Hemisphere, McGraw Hill, Washington, DC, 1980.

²⁹Rajagopalan, R. G., and Wilson, L. N., "A Finite Difference Approach Suitable for Solving the Flow Field of a Rotor," *Journal of Propulsion and Power*, Aug. 1987, (accepted for publication).

³⁰Vermeulen, P. E. J., and Bultjes, P. J. H., "Mathematics Modeling of Wake Interaction in Wind Turbine Arrays, Part 1: Description and Evaluation of the Mathematical Model," Netherlands Or-

ganization for Applied Scientific Research, the Netherlands, MT-TNO Rept. 81-01473.

³¹Worstell, M. H., "Aerodynamic Performance of the DOE/Sandia 17-m Vertical Axis Wind Turbine in the Two-Bladed Configuration," *Journal of Energy*, Vol. 5, Jan.-Feb. 1981, pp. 39-42.

³²Sheldahl, R. E., Klimas, P. C., and Feltz, L. V., "Aerodynamic Performance of a 5-m Diameter Darrieus Turbine," *Journal of Energy*, Vol. 4, No. 5, Sept.-Oct. 1980, pp. 227-232.


³³Maydew, R. C., and Klimas, P. C., "Aerodynamic Performance of Vertical and Horizontal Axis Wind Turbines," *Journal of Energy*, Vol. 5, No. 3, May-June 1981, pp. 189-190.

³⁴Strickland, J. H., and Goldman, A. L., "Preliminary Work Concerning the Near-Wake Structure of the Darrieus Turbine," *Journal of Energy*, Vol. 5, No. 2, March-April 1981, pp. 94-98.

³⁵Storza, P. M., Shervin, P., and Smorto, M., "Further Studies on Wind Turbine Generator Wakes," AIAA Paper, 1980.

³⁶Railly, J. W., "A Possible Saturation Criterion for Wind Energy Extraction," *Wind Engineering*, Vol. 1, No. 1, 1977, pp. 23-38.

Recommended Reading from the AIAA

Progress in Astronautics and Aeronautics Series . . . 

Single- and Multi-Phase Flows in an Electromagnetic Field: Energy, Metallurgical and Solar Applications

Herman Branover, Paul S. Lykoudis, and Michael Mond, editors

This text deals with experimental aspects of simple and multi-phase flows applied to power-generation devices. It treats laminar and turbulent flow, two-phase flows in the presence of magnetic fields, MHD power generation, with special attention to solar liquid-metal MHD power generation, MHD problems in fission and fusion reactors, and metallurgical applications. Unique in its interface of theory and practice, the book will particularly aid engineers in power production, nuclear systems, and metallurgical applications. Extensive references supplement the text.

TO ORDER: Write, Phone, or FAX: AIAA c/o TASC0,
9 Jay Gould Ct., P.O. Box 753, Waldorf, MD 20604
Phone (301) 645-5643, Dept. 415 ■ FAX (301) 843-0159

Sales Tax: CA residents, 7%; DC, 6%. For shipping and handling add \$4.75 for 1-4 books (call for rates for higher quantities). Orders under \$50.00 must be prepaid. Foreign orders must be prepaid. Please allow 4 weeks for delivery. Prices are subject to change without notice. Returns will be accepted within 15 days.

1985 762 pp., illus. Hardback
ISBN 0-930403-04-5
AIAA Members \$59.95
Nonmembers \$89.95
Order Number V-100